Morphological, Optical and Structural Properties of Zero-Net-Strained InGaAsP/InP Structures Grown by LP-MOVPE for 1.55μm Laser Applications

Wilson de Carvalho Jr[1]*, Ayrton André Bernussi[1], Mario Tosi Furtado[1], Angelo Luiz Gobbi[1], and Mônica Cotta[2]

1 - Fundação Centro de Pesquisa e Desenvolvimento em Telecomunicações
(Fundação CPqD) / Laboratório Nacional de Luz Sincrotron (LNLS)
2 - Laboratório de Pesquisa em Dispositivos (LPD) / DFA-Unicamp

Zero-Net-Strained (ZNS) InGaAsP/InGaAsP/InP Multi Quantum Wells (MQW) structures grown by Low Pressure Metalorganic Vapor Phase Epitaxy for 1.55μm laser applications were investigated using atomic force microscopy, photoluminescence spectroscopy and X-ray diffraction. The morphology exhibits a strong anisotropic and modulated behavior. The photoluminescence spectrum shows a broad emission band below the fundamental quantum well transition. The results indicate a strong influence of the growth rate, growth temperature and barrier composition on the surface morphology, and on the optical and structural properties of the ZNS structures. Ridge wave-guide ZNS-MQW laser structures grown at optimized conditions exhibited excellent electro-optic characteristics with low threshold current and high efficiency.

I   Introduction

InGaAsP quaternary alloy materials epitaxially grown on InP substrates have been extensively used to fabricate optoelectronic devices such as lasers, photodetectors, optical amplifiers and modulators for telecommunication applications. The introduction of a biaxial strain (ϵ) is able to modify the material electronic structure and this can be exploited to enhance the performance of optoelectronic devices. However, a strain relaxation process may occur if the layer thickness exceeds a critical value and misfit dislocations are created [1]. It is possible to compensate the total strain of a multi- quantum well (MQW) structure through the use of tensile strained barriers and compressive strained wells. Such structures are referred as zero-net-strained (ZNS). Nevertheless, the strain relaxation can occur prior to the misfit generation through elastic mechanisms. Also, the quaternary InGaAsP alloy may be affected by the miscibility gap [2,3], where a range of compositions and temperatures exist and the solid solution is energetically unstable. These mechanisms produce undulation at the interfaces, composition fluctuations, wavy morphologies and contribute to degrade the optical and structural properties of the grown layers [4-6]. High quality lattice matched GaInAs/InP and GaInAs/AlInAs superlattices with up to 100 periods, grown by MOVPE were obtained using low growth temperature and high growth rate [7].

In this work we present a systematic study of ZNS InGaAsP/InGaAsP/InP MQW heterostructures grown by Low Pressure Metalorganic Vapor Phase Epitaxy (LP- MOVPE) for 1.55μm laser applications. The effect of growth rate, growth temperature and barrier composition on the surface morphology and on the optical properties of ZNS structures were investigated using atomic force microscopy, photoluminescence spectroscopy and double crystal X-ray diffraction.

II   Experiment

The materials analyzed in this work were grown on InP:S (001) substrates by LP-MOVPE at the growth temperature (T_g) of 640 and 670°C under a reactor pressure of 70Torr. Arsine (AsH$_3$) and Phosphine (PH$_3$) hydrides were used as As and P source, respectively, and trimethylindium (TMIn) and triethylgallium (TEGa) organometallic compounds as In and Ga sources. Growth rates (R) of 2.5 Å/sec and 10Å/sec were used. The V/III ratios for barrier layers were close

---
*e-mail:junior@cpqd.com.br

to 300 and 100 for low and high growth rates, respectively.

The ZNS structures consisted of a InP buffer layer followed by the InGaAsP/InGaAsP MQW, with well number (N_w) ranging from 2 to 20 and tensile strained barriers ($\epsilon = -0.5\%$) with different band gaps ($1100 < \lambda_B < 1400$nm). In all studied samples, the well composition and the compressive biaxial strain were kept constant ($\lambda_{QW} = 1650$nm and $\epsilon = +1\%$). The barrier and well thicknesses were chosen in order to keep the total strain close to zero, with the emission wavelength at 1550nm. Samples with λ_B=1400nm were grown with the same As/P ratio in both well and barriers, reducing in this way the interdiffusion of As from the wells to barriers.

The samples were analyzed by Normasky interference optical microscopy, 300K and 77K photoluminescence (PL), double crystal X-ray diffraction (DCD) and Atomic Force Microscopy (AFM). InGaAsP alloy compositions were determined by combining the results of X-ray and PL measurements, using known data and band-offsets from the model-solid theory [8] and taking into account the amount of strain in the calculations.

III   Results and discussion

AFM scan of a ZNS-MQW structure grown with $N_w = 10$, $\lambda_B = 1300$nm, $T_g = 670°C$ with low and high growth rate is shown in Fig. 1. The morphology for low growth rate exhibits an anisotropic and modulated behavior (Fig. 1a). A strong thickness modulation occurs along [110] direction. The root mean square (rms) roughness, defined as the standard deviation of the data, is 5.8nm (approximately 20 mono-layers) and the thickness fluctuation, defined as the distance from valley to peak, is 35.6nm. For high growth rate (Fig. 1b) the thickness modulation almost disappeared and the surface is essentially flat, with a surface roughness less than one mono-layer. The waviness is dependent on the growth temperature, on the growth rate, on the number of wells and on the barrier composition. Reduced number of wells, higher growth temperatures, higher growth rates and barrier compositions grown outside the miscibility gap ($\lambda_B = 1100$ and 1400nm) are required to keep the morphology of ZNS structures flat and without waviness.
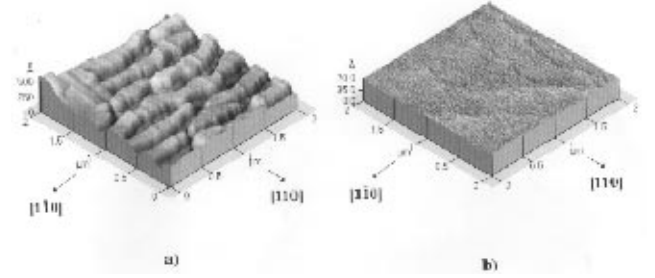

Figure 1. AFM image of a ZNS structure with $N_w = 10$, $\lambda_B = 1300$nm, $T_g = 670°C$ with a) low and b) high growth rate.

The low temperature PL spectra of ZNS samples grown with $N_w = 10$, $\lambda_B = 1300$nm, $T_g = 670°C$ and with low and high growth rates are shown in Fig. 2. Both PL spectra exhibited a very broad emission band (FWHM = 40meV) below the fundamental quantum well transition (FWHM = 16meV). The intensity ratio (I_{QW}/I_B) between the quantum well peak (labeled QW) and the broad emission band (B) depends on the number of wells, on the growth temperature, on the growth rate and on the barrier composition. The PL spectra of ZNS samples grown with the same structure but at lower temperatures and lower growth rates were dominated by the emission band B. At $T_g = 640°C$ and $R = 2.5Å/$sec. the relative intensity I_{QW}/I_B was as low as 0.08. Nevertheless, PL spectra of ZNS samples grown with $T_g = 670°C$ and R=10Å/sec. exhibited higher relative intensity I_{QW}/I_B of 2.12. The PL spectra of ZNS structures grown with a fixed growth temperature of 670°C, growth rate of 10Å/sec. and N_w=10, but with different barrier bandgap wavelength, showed a remarkable increase of the relative intensity I_{QW}/I_B as the barrier bandgap wavelength was varied from 1200 to 1400nm. The broad emission band B was not observed in the PL spectra of ZNS structures with $\lambda_B = 1400$nm and $N_w = 5$ or $N_w = 10$. This behavior can be tentatively explained by the use of constant As/P ratio in the wells and barriers (for λ_B=1400nm) which is known to reduce the thermal interdiffusion of group V species between barriers and wells. Also the barrier composition for λ_B=1400nm exhibits less phase separation, due to the miscibility gap, and consequently reduced alloy composition fluctuation is expected. Both effects result in improved interface quality. This observation was confirmed by AFM and X-ray diffraction measurements, where flat surface morphologies and intense and sharp satellite peaks were obtained in these samples, respectively. However, a further increase in the number of wells to $N_w = 15$ and $N_w = 20$ in ZNS structures grown with $\lambda_B = 1400$nm resulted in degradation of structural and optical properties of these samples. The surface morphology roughness increases, the

X- ray satellite peaks become broader and less intense and the relative intensity ratio I_{QW}/I_B decreases as N_w is increased from 15 to 20.
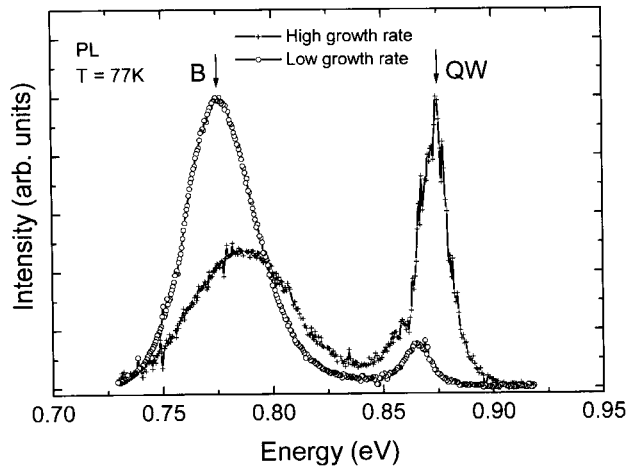

Figure 2. PL spectra of ZNS samples grown with low (circles) and high (crosses) growth rate. The arrows point to the broad band (B) and quantum well peak (QW).

The PL broad band emission B was not detected after the growth of a complete laser structure. The growth time of samples analyzed in this work is typically 40 min. A complete laser structure requires instead 3 hours of growth. This behavior may be explained if band B is attributed to defects generated at the interfaces between the tensile strained barriers and the compressive strained wells. During growth of the uppermost layers in the laser structure these defects are healed by the annealing process and the interface quality is improved. This results in the total suppression of the emission band B and a reduction of the well PL linewidth.

Double crystal X-ray diffraction, using Cu??1 radiation and (400) reflection, showed a strong influence of the growth rate on the structural properties of these samples, as shown in Fig. 3. The satellite intensities are strongly increased and became sharper for the sample grown at the higher growth rate. The n = +1 satellite diffraction linewidth is reduced by a factor of 1.9 when the growth rate is increased from 2.5 to 10Å/sec. These results suggest the presence of a strong interface undulation and/or alloy fluctuations in the structures grown at lower growth rate. Similar results were obtained for ZNS samples grown at different growth temperatures. Structures grown with lower temperatures (640°C) exhibited reduced I_{QW}/I_B values, low intensity and broad x-ray diffraction satellites when compared to samples grown at higher temperatures (670°C).
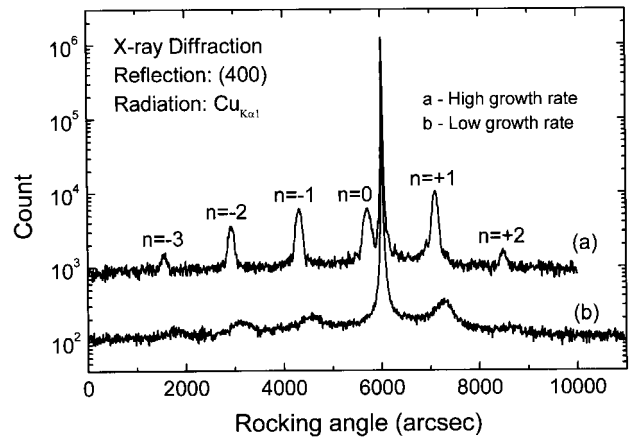

Figure 3. $Cu_{K\alpha1}$, (400) X-ray diffraction pattern of samples grown with a) low and b) high growth rates.

High quality ZNS structures, defined by a flat morphology, a high I_{QW}/I_B ratio in the PL spectrum and a high intensity and sharp x-ray diffraction satellites, were obtained with high growth temperatures and high growth rates. When the growth temperature is lowered the mobility of atoms at the surface is reduced. As a result, there is a reduction in the strain relaxation mechanism and less undulation is expected to occur [4]. However, lowering the growth temperature increases the miscibility gap of the quaternary alloy and a phase separation can take place [2,3], resulting in composition fluctuations of the tensile barrier layers. On the other hand, higher growth rate also decreases the mobility of atoms at the surface [9]. The interplay of these three mechanisms dominates the morphology and the optical and structural properties of ZNS structures. The predominance of one mechanism over the others is strongly influenced by the growth technique, amount of strain in the layers and the growth parameters.
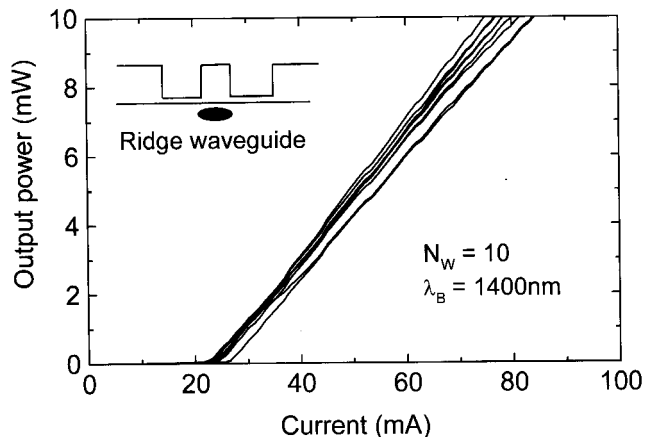

Figure 4. Pulsed light-current characteristics at T = 22°C of several quaternary MQW ZNS ridge lasers, grown with $T_g = 670^{\circ}$C, $N_w = 10$ and $\lambda_B = 1400$nm. The inset shows the ridge waveguide structure.

Ridge waveguide ZNS laser structures emitting at 1.55μm, with $N_w = 10$, grown at 670°C and at a high growth rate, exhibited excellent electro-optic characteristics. Fig. 4 shows pulsed light-current characteristics of several ridge waveguide ZNS lasers, with $\lambda_B = 1400$nm. The threshold current ranges from 23 to 26mA, with an external quantum efficiency of 0.2mW/mA. Similar results were obtained for structures grown with barriers of $\lambda_B = 1300$nm and $\lambda_B = 1200$nm.

IV   Conclusions

We presented an effective method to improve the material quality of InGaAsP/InGaAsP/InP MQW ZNS structures. Higher growth temperatures, higher growth rates and alloy compositions lying outside the miscibility gap are needed to dramatically suppress the wavy layer growth and to improve structural and optical characteristics of ZNS structures. ZNS ridge waveguide lasers exhibited excellent electro-optic characteristics with low threshold currents and high output external differential efficiencies.

References

[1] R. People and J.C. Bean, Appl. Phys. Lett. **47**, 322 (1985)

[2] B. de Cremoux, P. Hirtz and J. Ricciardi, Inst. Phys. Conf. Ser. N. **56**, 115 (1980).

[3] G. B. Stringfellow, J. Electronic Materials, **11**, 903 (1982).

[4] A. Ponchet, A. Le Corre, A. Godefroy, S. Salaun, and A. Poudoulec, J. Crystal Growth, **153**, 71 (1995).

[5] H. Chen, R. M. Feenstra, R.S. Goldman, C. Silfvenius and G. Landgren, Appl. Phys. Lett. **72**(14), 1727 (1998).

[6] R.W. Glew, K. Scarrot, A.T.R. Briggs, A.D. Smith, V.A. Wilkinson, X. Zhou and M. Silver, J. Crystal Growth, **145**, 764 (1994).

[7] R. Bhat, M. A. Koza, D. M. Hwang, K. Kash, C. Caneu and R. E. Nahory, J. Cryst. Growth, **110**, 353 (1991).

[8] C. G. Van de Walle, Physical Review B, **39**(3), 1871 (1989).

[9] N. Y. Jin-Phillipp, F. Phillipp, T. Marschner and W. Stolz, J. of Material Science: Materials in Electronics **8**, 289 (1997).